Inorganic Chemistry
Cite This: Inorg. Chem. 2018, 57, 9720−9727
Forum Article
pubs.acs.org/IC

Reactivity of Two-Electron-Reduced Boron Formazanate Compounds with Electrophiles: Facile N−H/N−C Bond Homolysis Due to the Formation of Stable Ligand Radicals

Ranajit Mondol and Edwin Otten*

Stratingh Institute for Chemistry, University of Groningen, Nijenborgh 4, 9747 AG Groningen, The Netherlands

Supporting Information

ABSTRACT: The reactivity of a boron complex with a redox-active formazanate ligand, $LBPh_2$ [L = PhNNC(*p*-tol)NNPh], was studied. Two-electron reduction of this main-group complex generates the stable, nucleophilic dianion $[LBPh_2]^{2-}$, which reacts with the electrophiles BnBr and H_2O to form products that derive from ligand benzylation and protonation, respectively. The resulting complexes are anionic boron analogues of leucoverdazyls. N−C and N−H bond homolysis of these compounds was studied by exchange NMR spectroscopy and kinetic experiments. The weak N−C and N−H bonds in these systems derive from the stability of the resulting borataverdazyl radical, in which the unpaired electron is delocalized over the four N atoms in the ligand backbone. We thus demonstrate the ability of this system to take up two electrons and an electrophile ($E^+ = Bn^+, H^+$) in a process that takes place on the organic ligand. In addition, we show that the $[2e^-/E^+]$ stored on the ligand can be converted to $E^\bullet$ radicals, reactivity that has implications in energy storage applications such as hydrogen evolution.

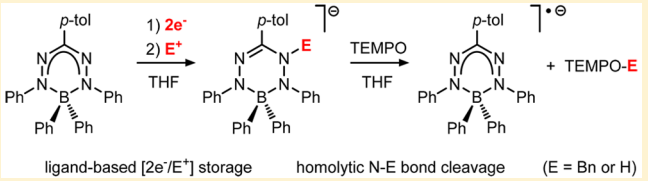

INTRODUCTION

A key feature in the reactivity of molecular complexes with transition-metal centers is their ability to change oxidation states via electron-transfer reactions. This has allowed the development of a large variety of redox-based catalytic transformations that are of importance in the synthesis of organic molecules, polymers, and materials. Often these reactions rely on two-electron steps (e.g., oxidative addition/reductive elimination). Also, in energy applications, interconversion between redox states in simple small molecules is relevant, and catalysis is imperative to allow high reaction rates and to control product selectivity. With the transition from a fossil-based to a renewable energy supply, a key challenge is to develop reliable, cheap methods to convert and store sustainable energy into chemicals ("solar fuels").[1] Examples of chemical reactions for energy storage include CO_2 reduction to CO, formic acid, or methanol,[2] the interconversion between N_2 and NH_3,[3] and H_2O splitting.[4] In the latter, the oxidation of H_2O ($2H_2O \rightarrow O_2 + 4H^+ + 4e^-$)[5] provides protons and electrons that can be used to drive a multitude of subsequent reactions, either directly or via the formation of H_2. The high thermodynamic and kinetic stability of several of these molecules (e.g., CO_2 and N_2) and the multistep, multielectron nature of their transformation place significant demands on the catalyst design: catalysts should be stable in a variety of redox states, be able to efficiently transform a multitude of intermediates en route to the final product(s), and at the same time have low activation barriers for each individual step in the reaction sequence. Against this backdrop, it is perhaps not surprising that there is much interest in molecular catalysts for energy applications because these offer the possibility of tuning the catalyst properties with great precision via rational molecular design and can provide detailed insight into the reaction mechanism(s) at play.

The majority of synthetic molecular catalysts that operate via elementary steps involving changes in the oxidation state are proposed to do so by changing the formal oxidation state of the central metal atom. In contrast, Nature often uses metalloenzymes in which there is an organic redox-active cofactor adjacent or bound to the active site. The role of these redox-active moieties is to accumulate redox equivalents that can subsequently be used by the metalloenzyme to perform challenging multielectron transformations. Examples of such metalloenzymes include galactose oxidase[6] and cytochrome P450,[7] which store redox equivalents in the organic ligand scaffold to ultimately perform two-electron oxidation of alcohols and aliphatic CH bonds, respectively. Inspired by these enzymatic systems, there is increasing interest in the chemistry of synthetic catalysts with redox-active ligands.[8] The electronic structure of such complexes, which underpins our understanding of the reactivity, is only beginning to be uncovered in recent years. As an example, iron porphyrin complexes that perform electrocatalytic CO_2 reduction at the formal Fe^0 potential have recently been shown to consist of an intermediate-spin Fe^{II} center that is antiferromagnetically coupled to a two-electron-reduced porphyrin diradical; the

Special Issue: Applications of Metal Complexes with Ligand-Centered Radicals

Received: January 12, 2018
Published: February 15, 2018

DOI: 10.1021/acs.inorgchem.8b00079
Inorg. Chem. 2018, 57, 9720−9727

Chart 1

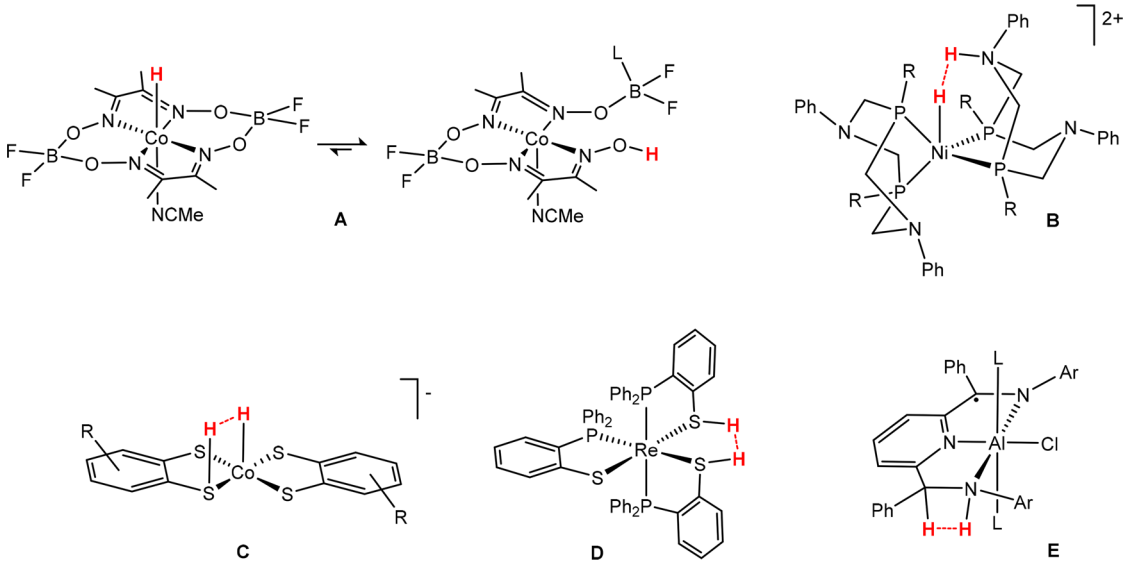

reducing equivalents in this catalyst species thus reside on the organic ligand.[9] Moreover, electrocatalytic CO_2 reduction using a porphyrin complex with a redox-innocent Zn^{II} ion was recently reported,[10] further highlighting the importance of ligand-based redox reactions in these systems. Recent studies on azo-containing pincer ligands have shown that also alcohol dehydrogenation can be catalyzed via a pathway that involves a reduced azo moiety.[11] Similarly, studies on molecular electrocatalysts for the hydrogen evolution reaction (HER) have identified several systems in which the mechanism does not involve "traditional" metal hydride intermediates;[12] instead, the organic ligand is proposed to be involved as the locus of reduction, protonation, or both. Thus, the assembly of two protons and two electrons as required for H_2 production requires a delicate interplay between the reactivity of the metal center and that of the ligand. Illustrative examples include cobaloximes[13] (Chart 1, **A**) and related compounds,[14] for which there has been considerable debate on the intermediates that lead to H_2 formation,[15,16] and nickel diphosphine complexes with a "pendant" proton-relay site (Chart 1, **B**).[17] In addition, hydrogen evolution catalysts are known with "redox-active" ligands: homogeneous cobalt dithiolene compounds have been pioneered by Holland and Eisenberg (Chart 1, **C**),[18−20] and these were recently extended to heterogeneous systems[21] and their mechanisms studied computationally.[22] Recent work from Grapperhaus and co-workers identified homogeneous proton reduction catalysts that proceed via ligand-centered reactions in which metal hydride species are not involved (Chart 1, **D**),[23] and also nickel porphyrin HER catalysts have been shown to undergo reduction/protonation to lead to an organic hydride as the key intermediate generated by ligand-based [$2e^-/H^+$] reactivity.[24] In addition to catalysts containing transition-metal centers, examples have been reported of main-group complexes that are active in hydrogen evolution,[25] as illustrated by Berben's aluminum complexes with reduced pyridinediimine ligands (Chart 1, **E**).

The mechanistic ambiguities in (electro)catalysis and the new types of reactivities that can result with metal complexes that contain redox-active ligands make these interesting systems for further exploration. Intrigued by work from the Hicks group on formazanate ligands as nitrogen-rich, redox-active analogues of the well-known β-diketiminates,[26] our group has started a research program to explore the coordination chemistry, redox behavior, and reactivity of complexes with formazanate ligands.[27] Although some early reports on related complexes exist,[28,29] it is only recently that interest in this class of ligands has gained momentum. Concurrent with our work, the Gilroy group and others have reported related complexes with formazanate ligands and studied the properties of these compounds[30,31] and materials derived thereof.[32] Previously, we studied ligand-based reductions in boron formazanate compounds and showed that both one- and two-electron-reduced products can be obtained (Scheme 1).[33] For the boron

Scheme 1. Synthesis of One- and Two-Electron-Reduced Boron Formazanate Compounds and Their Conversion to BN Heterocyclic Products via an N-Heterocyclic Boron(I) Carbenoid Intermediate

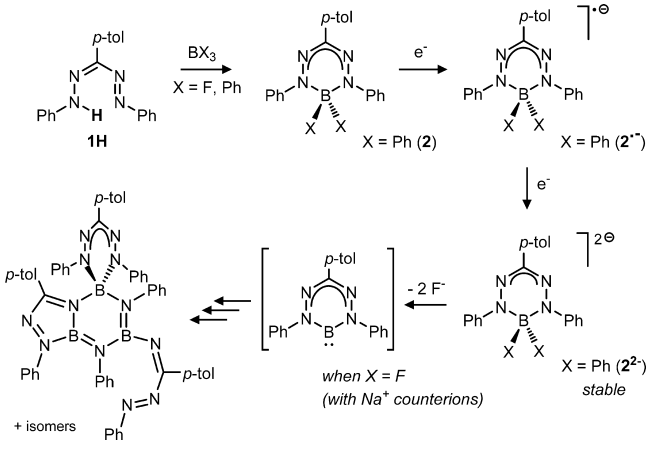

difluoride derivative, two-electron reduction leads to the elimination of 2 equiv of F^- and the formation of a boron carbenoid intermediate, the fate of which is ultimately a series of B_3N_3 heterocyclic products that incorporate the boron formazanate fragment (Scheme 1).[34]

In this Forum Article, we present boron complexes with the formazanate ligand L [$LBPh_2$ (**2**), where L = [PhNNC(*p*-

DOI: 10.1021/acs.inorgchem.8b00079
Inorg. Chem. 2018, 57, 9720−9727

tol)NNPh]$^-$] and explore the nucleophilic reactivity of the corresponding two-electron-reduced complex [$LBPh_2$]$^{2-}$ ($\mathbf{2}^{2-}$) with the electrophiles BnBr and H_2O. The products are group 13 analogues of leucoverdazyls (tetrahydro-1,2,4,5-tetrazines). Our results demonstrate that, starting from neutral **2**, the sequential "storage" of two electrons and 1 equiv of an electrophile (E^+ = Bn^+, H^+) occurs in this main-group compound, an overall [$2e^-/E^+$] process that takes place exclusively at the organic ligand. The ability of the products to subsequently undergo homolytic N−H and N−C bond cleavage was investigated by exchange NMR spectroscopy and kinetic experiments.

RESULTS AND DISCUSSION

The ligand **1H**, its corresponding boron complex **2**, and the dianion $\mathbf{2}^{2-}$ were prepared as reported previously (Scheme 1).[33c] Treatment of the two-electron-reduced, dianionic boron formazanate compound $\mathbf{2}^{2-}$ with BnBr on an NMR scale in tetrahydrofuran (THF)-d_8 resulted in the clean formation of a new compound. The appearance of a set of (broad) diastereotopic protons at 3.78 and 3.42 ppm in the ^{1}H NMR spectrum is indicative of a benzyl group attached to an N atom of the formazanate ligand, and the product is formulated as the ligand-benzylated compound [$^{Bn}LBPh_2$]$^-$ ($^{Bn}\mathbf{3}^-$; Scheme 2).

Scheme 2. Synthesis of Compounds $^{Bn}\mathbf{3}^-$ and $^{H}\mathbf{3}^-$

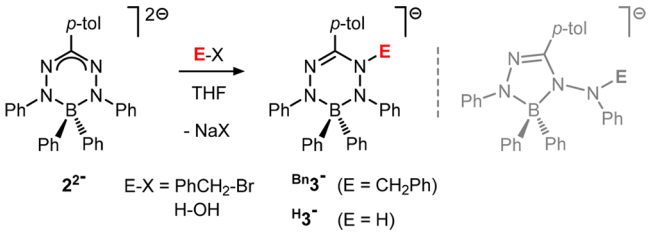

Repeating the reaction on a preparative scale allowed the isolation of $^{Bn}\mathbf{3}^-$ (as its sodium salt) in 92% yield as a waxy green solid upon precipitation with hexane. NMR analysis of isolated $^{Bn}\mathbf{3}^-$ at room temperature in a THF-d_8 solution shows fluxional behavior, with several resonances being broadened. A variable-temperature NMR study (500 MHz, THF-d_8) in the temperature range between −30 and +70 °C shows that the broadening of the diastereotopic benzyl CH_2 resonances is due to chemical exchange: two sharp doublets are observed at −25 °C (3.79 and 3.38 ppm) that are mutually coupled with $^2J_{HH}$ = 15.3 Hz. At 70 °C, these signals are coalesced and appear as a sharp singlet at 3.69 ppm. Resonances due to the phenyl groups bound to boron are also exchange-broadened, with two distinct BPh resonances observed at low temperature that coalesce to a single set for the BPh_2 moiety at temperatures >65 °C. These observations are taken as an indication that in the highly congested structure of $^{Bn}\mathbf{3}^-$ the rotation around the N−CH_2Ph bond is "geared" to rotation of the BPh moieties. The *p*-H atoms of the inequivalent NPh rings in $^{Bn}\mathbf{3}^-$ are observed at 6.16 and 6.07 ppm, and the former shows additional coupling, the magnitude of which is temperature-dependent. We attribute this feature to through-space interactions with protons of the *N*-benzyl ring due to their close proximity. The ^{11}B NMR resonance at 1.16 ppm is indicative of a four-coordinate B center, supporting the assignment of $^{Bn}\mathbf{3}^-$ as a boron diphenyl complex with a benzylated formazanate fragment. The reaction of $\mathbf{2}^{2-}$ with BnBr is best regarded as a S_N2-type nucleophilic substitution, with the highly charged formazanate ligand in $\mathbf{2}^{2-}$ acting as the nucleophile.

Similarly, the reaction of $\mathbf{2}^{2-}$ with 1 equiv of H_2O results in the clean formation of the corresponding protonated product $^{H}\mathbf{3}^-$ with precipitation of NaOH (Scheme 2). The diagnostic N−H resonance of $^{H}\mathbf{3}^-$ is found at 5.04 ppm in the ^{1}H NMR spectrum, while the ligand and BPh_2 groups in $^{H}\mathbf{3}^-$ are similar to those in $^{Bn}\mathbf{3}^-$ with two upfield N−Ph NMR resonances due to *p*-H at 6.12 and 6.08 ppm. The similarity of the NMR spectral data for $^{H}\mathbf{3}^-$ and $^{Bn}\mathbf{3}^-$ suggests that they have comparable structures, with the same site of attack in the formazanate ligand for both electrophiles. The compounds are invariably obtained as oily materials, but storage of a sample of $^{Bn}\mathbf{3}^-$ (as a green oil) on THF/hexane at −30 °C for several days allowed the oil to solidify and form forest-green crystals. Unfortunately, the crystals melt again when taken out of the mother liquor, and we were unable to obtain structural data by X-ray crystallography. Although, in principle, two structural types can be plausibly formulated for these compounds (six- and five-membered ring isomers; see Scheme 2), NMR spectroscopy is most consistent with a six-membered cyclic structure (shown as $^{Bn/H}\mathbf{3}^-$). In particular, two-dimensional NOESY NMR spectroscopy showed cross-peaks of similar intensity between the N−H resonance and the *o*-H signals of both the *p*-tolyl and one of the N−Ph rings, as expected for structures $\mathbf{3}^-$. In addition, a comparison of the empirical and density functional theory (DFT)-calculated NMR chemical shifts is most consistent with six-membered chelate rings (see Supporting Information for details). Finally, six-membered-ring carbon-based analogues of $\mathbf{3}^-$ (leucoverdazyls) are well-established in the literature, and the reactivity of $^{Bn/H}\mathbf{3}^-$ (vide infra) is similar to that in the organic analogues.[35] On the basis of these considerations, we propose that compounds $^{Bn/H}\mathbf{3}^-$ have the structures shown in Scheme 2. Related charge-neutral boron hydride compounds were prepared by the thermolysis of (formazanate)BH_2 compounds. In these systems, intramolecular transfer of a hydride from the BH moiety to the formazanate ligand occurs at ca. 100 °C, which also formally involves a [$2e^-/H^+$] modification of the ligand, but this is accompanied by N−N bond cleavage as a result of a second hydride being transferred.[36] The current approach of sequential two-electron reduction, followed by external electrophile addition, leads to the clean formation of "borataleucoverdazyls", a class of compounds that to the best of our knowledge have not been prepared previously.

The UV/vis spectra of compounds $^{H}\mathbf{3}^-$ and $^{Bn}\mathbf{3}^-$ in THF are similar and show absorption maxima at 400 and 395 nm, respectively, presumably because of a $\pi \rightarrow \pi^*$ transition in the (localized) N=C bond (Figure S5). These bands are shifted to higher energies in comparison to the intense $\pi \rightarrow \pi^*$ transition band in compounds with fully delocalized formazanate ligands (e.g., λ_{max} = 500 nm in **2**) but in the same range as that found in complexes with the same oxidation state of the ligand (L^{3-}), such as the precursor $\mathbf{2}^{2-}$ (λ_{max} = 389 nm).[33c]

In the context of proton reduction chemistry, it was of interest to evaluate the further reactivity of these compounds. The anionic boron compounds $^{Bn/H}\mathbf{3}^-$ are unreactive toward an additional 1 equiv of electrophile (BnBr or H_2O) but do react with strong acids such as *p*-toluenesulfonic acid. The NMR spectra of these reactions, however, show a complex mixture, and in no case could the formation of H_2 (or BnH) be ascertained. The lack of controlled further reactivity of $^{Bn/H}\mathbf{3}^-$ (other than decomposition to unidentified products when

DOI: 10.1021/acs.inorgchem.8b00079
Inorg. Chem. 2018, 57, 9720−9727

Scheme 3

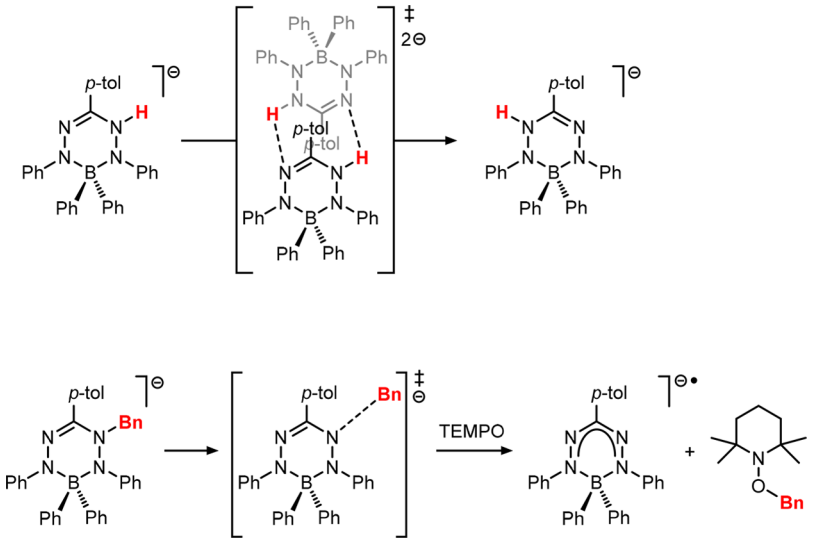

reacted with strong acid) might indicate that these anionic compounds are not sufficiently basic (nucleophilic) to react with mild electrophiles. Although these preliminary data suggest that in the present system accumulation of the [2e⁻/2H⁺] equivalents required for proton reduction is not feasible, we anticipate that changes in the ligand substitution pattern and/or the use of acids of intermediate pK_a might solve these problems. It is important to note that ligand-centered reactions that accumulate two electrons and a proton ([2e⁻/H⁺]) were recently shown to generate an organic "hydride equivalent" in the case of a nickel "hangman" porphyrin that is able to release H_2 following a second protonation step.[24] In this system, the sequence of reduction/protonation events (and thus the mechanism of H_2 evolution catalysis) was shown to be highly dependent on the acid strength. Our results demonstrate that a similar accumulation of [2e⁻/H⁺] can take place in the boron complex **2**, but the reactivity of the resulting organic (ligand) "hydride" needs further exploration.

Given the similarity of the anionic compounds $^{Bn/H}\mathbf{3}^-$ to neutral leucoverdazyls (1,2,3,4-tetrahydro-1,2,4,5-tetrazines), we became interested in cleavage of the N−H and N−C bonds in these systems. Hicks and co-workers recently described that coordination to a Ru center weakens the N−C bond in an *N*-benzyltetrazine via metal−ligand noninnocence and leads to homolysis that is ca. 40 times faster than that without metal bound.[37] The influence of main-group or transition-metal elements incorporated *into* these heterocyclic structures has not been studied before, but homolytic cleavage is expected to generate the radical anions $\mathbf{2}^{\bullet-}$, which contain ligand-based radicals and are relatively stable due to delocalization of the unpaired electron over all four N atoms (Figure S14).[33c,35b] For the "borataleucoverdazyl" $^{H}\mathbf{3}^-$, its lack of symmetry (C_1) results in inequivalent N−Ph groups, and 2D EXSY NMR spectroscopy in a THF-d_8 solution shows chemical exchange cross-peaks between the well-separated *o*-H resonances of these rings, which is the result of net H-atom transfer between the two "internal" N atoms in the ligand backbone. The mechanism of H-atom transfer can occur either via a dissociative mechanism (N−H bond homolysis) or intramolecularly via a bimolecular (associative) pathway. To probe the mechanism of H-atom transfer, the exchange kinetics were measured by 2D EXSY NMR spectroscopy in the temperature range 10−65 °C. Subsequent Eyring analysis afforded the activation parameters as $\Delta H^{\ddagger}$ = 44.2 ± 0.9 kJ·mol^{-1} and $\Delta S^{\ddagger}$ = −93 ± 3 J·mol^{-1}·K^{-1} (see the Supporting Information for details). The large, negative activation entropy is in agreement with a bimolecular mechanism, and the activation enthalpy is too low for (homolytic) N−H bond dissociation as the rate-determining step. An estimation of the N−H bond dissociation energy using DFT calculations (via geometry optimizations at increasing N−H distances) reveals a value of ca. 275 kJ·mol^{-1}, in agreement with the experimental values for leucoverdazyls (281−307 kJ·mol^{-1}).[38] These arguments support a (symmetrical) exchange pathway via the bimolecular mechanism shown in Scheme 3.

The reaction of $^{H}\mathbf{3}^-$ with TEMPO in THF is fast and generates $\mathbf{2}^{\bullet-}$ according to electron paramagnetic resonance (EPR) spectroscopy by comparison to an authentic sample. Despite the presence of paramagnetic species, the ^{1}H NMR spectra show relatively sharp resonances for $^{H}\mathbf{3}^-$ and TEMPO-H, and complete (>95%) consumption of the starting material for a 1:1 mixture indicates that the N−H bond in $^{H}\mathbf{3}^-$ is weaker than that in TEMPO-H, for which a bond dissociation free energy of 270−280 kJ·mol^{-1} in organic solvents has been reported.[39]

In contrast to $^{H}\mathbf{3}^-$, the benzyl analogue $^{Bn}\mathbf{3}^-$ does not show 2D EXSY NMR cross-peaks even at elevated temperature (75 °C). This likely is due to a change in the mechanism, with (dissociative) homolytic cleavage of the N−C bond now operative. To obtain insight into the N−C(Bn) bond dissociation energy, the kinetics of benzyl transfer from $^{Bn}\mathbf{3}^-$ to TEMPO were measured in the temperature range between 55 and 85 °C. To effectively trap the Bn$^{\bullet}$ radical formed, kinetic experiments were carried out in the presence of 20 equiv of TEMPO. Monitoring the reaction at regular time intervals by ^{1}H NMR spectroscopy showed clean exponential decay of the starting material and the concomitant appearance of TEMPO-Bn. Eyring analysis afforded the activation parameters as $\Delta H^{\ddagger}$ = 121 ± 5 kJ·mol^{-1} and $\Delta S^{\ddagger}$ = 77 ± 14 J·mol^{-1}·K^{-1} (see the Supporting Information for details). Under similar conditions, transfer of the 4-fluorobenzyl group in $^{F\text{-}Bn}\mathbf{3}^-$ to TEMPO was evaluated, which was shown to have activation parameters of $\Delta H^{\ddagger}$ = 107 ± 3 kJ·mol^{-1} and $\Delta S^{\ddagger}$ = 36 ± 9 J·mol^{-1}·K^{-1}. In agreement with rate-determining N−C(Bn) bond homolysis,

DOI: 10.1021/acs.inorgchem.8b00079
Inorg. Chem. 2018, 57, 9720−9727

the activation entropy is large and positive, and $\Delta H^{\ddagger}$ can be taken as an approximation of the N−C bond dissociation enthalpy.[37,40] The $\Delta H^{\ddagger}$ values of 121 ± 5 and 107 ± 7 kJ·mol^{-1} for $^{Bn}\mathbf{3}^{-}$ and $^{F\text{-}Bn}\mathbf{3}^{-}$, respectively, are somewhat smaller than that in pure carbon-based *N*-alkyl-substituted benzyltetrazines[37,41] and fall in the lower range of C−O bond dissociation energies in the well-studied alkoxyamines[40,42] or Ti−O bond dissociation energies in titanocene(IV) complexes derived from nitroxyl radicals.[43]

CONCLUDING REMARKS

In conclusion, this work shows that the ligand in boron formazanate complexes is reactive and can be used to accumulate [2e$^-$/E$^+$] equivalents (E$^+$ = Bn$^+$, H$^+$), a step that has precedent in nontraditional hydrogen evolution catalysts (i.e., those not going through metal hydride intermediates; E$^+$ = H$^+$).[24] Although preliminary attempts to elicit "organohydride" reactivity in $^{H}\mathbf{3}^{-}$ by protonation, a reaction relevant to hydrogen evolution, were not successful, compounds $^{Bn/H}\mathbf{3}^{-}$ are shown to have weak N−H/N−C bonds that are readily cleaved homolytically. Our results complement Hicks' observation that N−C bond homolysis in coordinated leucoverdazyls may be controlled by metal−ligand covalency and consequent spin delocalization onto the metal center. The incorporation of an element other than C (here, B) in the six-membered ring of leucoverdazyls similarly allows modulation of the homolytic N−C and N−H bond cleavage energies. The weak N−C and N−H bonds in these systems is a result of the stability of the resulting boron formazanate radical ("borataverdazyl") species. Having established the synthesis and characterization of "borataleucoverdazyls", we are currently exploring ligand-substituent effects on the reactivity of these compounds. In general, we anticipate that the ability to influence the basicity, radical stability, and N−H/N−C bond strength of compounds containing the formazanate ligand, either via substituent effects or by the incorporation of different central elements (main group or transition metal), can be used to modulate the reactivity and steer it away from the observed radical reactions (H$^{\bullet}$/Bn$^{\bullet}$ transfer) toward multielectron reactions (e.g., [2e$^-$/2H$^+$]). These reactions are of fundamental importance, for example, in electrocatalytic hydrogen evolution, and we are actively working toward applying our systems in this area.

EXPERIMENTAL SECTION

General Considerations. All manipulations were carried out under a nitrogen or an argon atmosphere using standard glovebox, Schlenk, and vacuum-line techniques. Toluene and hexane (Aldrich, anhydrous, 99.8%) were passed over columns of Al_2O_3 (Fluka), BASF R3-11-supported copper oxygen scavenger, and molecular sieves (Aldrich, 4 Å). THF (Aldrich, anhydrous, 99.8%) was dried by percolation over columns of Al_2O_3 (Fluka). Compounds $^{H}\mathbf{3}^{-}$, $^{Bn}\mathbf{3}^{-}$, and $^{F\text{-}Bn}\mathbf{3}^{-}$ are highly air-sensitive, and the solvents (THF and hexane) used for their preparation and characterization were additionally dried on a sodium/potassium alloy and subsequently vacuum-transferred and stored under nitrogen. All solvents were degassed prior to use and stored under nitrogen. THF-d_8 (Sigma-Aldrich) was vacuum-transferred from a sodium/potassium alloy and stored under nitrogen. Compound $\mathbf{2}^{2-}$ (as its disodium salt, [(PhNNC(p-tol)NNPh)BPh$_2$]-[Na$_2$(THF)$_6$]) was synthesized according to a published procedure.[33c] NMR spectra were recorded on a Varian Mercury 400, Inova 500, or Bruker 600 spectrometer. The ^{1}H and ^{13}C NMR spectra were referenced internally using the residual solvent resonances and reported in ppm relative to TMS (0 ppm); *J* is reported in hertz. The assignments of NMR resonances were aided by COSY, NOESY, HSQC, and HMBC experiments using standard pulse sequences. UV/vis spectra were recorded in a THF solution (~10^{-3} M) in a quartz cuvette using an AVANTES AvaSpec-2048 spectrometer. Samples for elemental analyses were sent to Kolbe Microanalytical Laboratory (Mülheim an der Ruhr, Germany). However, despite our best efforts, no satisfactory analysis data could be obtained for these compounds, which is likely due to their highly air-sensitive nature and/or to the fact that these compounds are oily and therefore still contain residual solvent and/or (unknown) impurities. It should be noted, however, that NMR spectroscopy indicates that compounds $^{H/Bn}\mathbf{3}^{-}$ are formed cleanly (>90% by integration relative to an internal standard).

Synthesis of [^{H}LBPh$_2$]Na(THF)$_2$ ($^{H}\mathbf{3}^{-}$). Compound $\mathbf{2}^{2-}$ (400 mg, 0.598 mmol) was dissolved in 2 mL of THF in a Schlenk tube inside the glovebox. To this was added 1 equiv of H$_2$O (as a dilute solution in THF), which caused the color to change from orange to purple-red. After the mixture was stirred for 1 h, all of the volatiles were removed under reduced pressure and the crude product was washed with hexane (3 × 2 mL). Subsequently, drying under vacuum gave compound $^{H}\mathbf{3}^{-}$ as an oily green material (339 mg, 0.524 mmol, 87%). ^{1}H NMR (500 MHz, THF-d_8, −5 °C): δ 7.79 (d, *J* = 8.0 Hz, 2H, *p*-tol *o*-H), 7.39 (d, *J* = 7.1 Hz, 4H, BPh *o*-H), 7.01 (d, *J* = 8.0 Hz, 2H, *p*-tol *m*-H), 6.97 (d, *J* = 7.9 Hz, 2H, N(2)Ph *o*-H), 6.91 (t, *J* = 7.1 Hz, 4H, BPh *m*-H), 6.85 (t, *J* = 7.1 Hz, 2H, BPh *p*-H), 6.67−6.52 (overlapped, 6H, N(1)Ph (*o* + *m*)-H and N(2)Ph *m*-H), 6.12 (t, *J* = 7.0 Hz, 1H, N(2)Ph *p*-H), 6.08 (t, *J* = 6.8 Hz, 1H, N(1)Ph *p*-H), 5.04 (s, 1H, NCNH), 3.62 (m, 10H, THF), 2.28 (s, 3H, *p*-tol CH$_3$), 1.78 (m, 10H, THF). ^{11}B NMR (128.0 MHz, THF-d_8, 25 °C): δ 0.4 (s). ^{13}C NMR (125 MHz, THF-d_8, −5 °C): δ 156.39 (BPh *ipso*-C), 155.14 (N(1)Ph *ipso*-C), 154.55 (N(2)Ph *ipso*-C), 138.48 (NCN), 136.20 (*p*-tol CNCN), 135.88 (BPh *o*-CH), 135.62 (*p*-tol CCH$_3$), 128.75 (*p*-tol *m*-CH), 127.40 (N(2)Ph *m*-CH), 126.86 (BPh *m*-CH), 126.78 (N(1)Ph *o*-CH), 125.47 (*p*-tol *o*-CH), 124.33 (BPh *p*-CH), 118.94 (N(2)Ph *o*-CH), 117.35 (N(1)Ph *m*-CH), 113.93 (N(2)Ph *p*-CH), 113.31 (N(1)Ph *p*-CH), 68.30 (THF), 26.44 (THF), 21.41 (*p*-tol CH$_3$).

Synthesis of [^{Bn}LBPh$_2$]Na(THF)$_2$ ($^{Bn}\mathbf{3}^{-}$). Compound $\mathbf{2}^{2-}$ (400 mg, 0.498 mmol) was dissolved in 2 mL of THF in a Schlenk tube inside a glovebox. To this was added 1 equiv of benzyl bromide, which caused the color to change from orange to purple-red. After the mixture was stirred for 1 h, all of the volatiles were removed under reduced pressure and the crude product was washed with hexane (3 × 2 mL). Subsequently, drying under vacuum gave compound $^{Bn}\mathbf{3}^{-}$ as an oily green material (292 mg, 0.450 mmol, 92%). ^{1}H NMR (600 MHz, THF-d_8, 10 °C): δ 7.83 (d, *J* = 8.1 Hz, 2H, *p*-tol *o*-H), 7.69 (d, *J* = 6.9 Hz, 2H, B(1)Ph *o*-H), 7.09 (t, *J* = 7.0 Hz, 2H, B(1)Ph *m*-H), 7.05−6.98 (overlapped, 6H, (benzyl)Ph *o*-H, B(2)Ph *o*-H, and *p*-tol *m*-H), 6.97 (t, *J* = 7.0 Hz, 1H, B(1)Ph *p*-H), 6.94 (d, *J* = 6.4 Hz, 2H, N(1)Ph *o*-H), 6.87−6.79 (m, 3H, (benzyl)Ph (*m* + *p*)-H), 6.57−6.53 (overlapped, 5H, N(1)Ph *m*-H and B(2)Ph (*m* + *p*)-H), 6.47−6.45 (m, 4H, N(2)Ph (*o* + *m*)-H), 6.17−6.14 (m, 1H, N(2)Ph *p*-H), 6.07 (t, *J* = 7.0 Hz, 1H, N(1)Ph *p*-H), 3.78 (d, *J* = 15.3 Hz, 1H, benzyl CH$_2$), 3.62 (m, 8H, THF), 3.42 (d, *J* = 15.3 Hz, 1H, benzyl CH$_2$), 2.28 (s, 3H, *p*-tol CH$_3$), 1.78 (m, 8H, THF). ^{11}B NMR (128.3 MHz, THF-d_8, 25 °C): δ 1.16 (s). ^{13}C NMR (150 MHz, THF-d_8, 10 °C): δ 158.66 (N(2)Ph *ipso*-C), 155.48 (B(1,2)Ph *ipso*-C), 154.07 (N(1)Ph *ipso*-C), 142.34 (NCN), 141.66 ((benzyl)Ph *ipso*-C)), 137.67 (NCN-*p*-tol *ipso*-C), 137.17 (B(1)Ph *o*-CH), 137.08 (B(2)Ph *o*-CH), 135.25 (*p*-tol-CH$_3$ *ipso*-C), 129.62 ((benzyl)Ph *o*-CH), 128.77 (*p*-tol *m*-CH), 127.41 (*p*-tol *o*-CH), 127.34 ((benzyl)Ph *p*-CH), 126.59 (B(2)Ph *m*-CH), 126.33 (B(1)Ph *m*-CH), 126.14 (N(2)Ph *o*-CH), 125.69 (B(2)Ph *p*-CH), 125.64 ((benzyl)Ph *m*-CH), 124.03 (B(1)Ph *p*-CH), 123.77 (N(2)Ph *p*-CH), 123.40 (N(1)Ph *m*-CH), 118.56 (N(1) Ph *o*-CH), 116.37 (N(2)Ph *p*-CH), 113.78 (N(1)Ph *p*-CH), 68.29 (THF), 26.45 (THF), 21.37 (*p*-tol CH$_3$).

Synthesis of [$^{F\text{-}Bn}$LBPh$_2$]Na(THF)$_2$ ($^{F\text{-}Bn}\mathbf{3}^{-}$). Compound $\mathbf{2}^{2-}$ (100 mg, 0.12 mmol) was dissolved in 1 mL of THF in a Schlenk tube inside a glovebox. To this was added 1 equiv of 4-fluorobenzyl bromide, which caused the color to change from orange to purple-red. After the mixture was stirred for 1 h, all of the volatiles were removed under reduced pressure and the crude product was washed with hexane (3 × 2 mL). Subsequently, drying under vacuum gave compound $^{F\text{-}Bn}\mathbf{3}^{-}$ as an oily purple-red material (72 mg, 0.095 mmol, 79%). ^{1}H NMR (400

DOI: 10.1021/acs.inorgchem.8b00079
Inorg. Chem. 2018, 57, 9720−9727

MHz, THF-d_8, 25 °C): δ 7.81 (d, J = 8.1 Hz, 2H, p-tol o-H), 7.69 (bs, 2H, BPh o-H), 7.10 (bs, 3H, BPh (m + p)-H), 7.02 (overlapped, 4H, BPh o-H and p-tol m-H), 7.00−6.96 (m, 2H, (benzyl)Ph o-H), 6.95 (d, J = 8.1 Hz, 2H, N(1)Ph o-H), 6.55 (overlapped, 7H, (benzyl)Ph m-H, N(1)Ph m-H, and BPh (m + p)-H), 6.47−6.45 (m, 4H, N(2)Ph (o + m)-H), 6.16 (m, 1H, N(2)Ph p-H), 6.07 (t, J = 7.1 Hz, 1H, N(1)Ph p-H), 3.75 (d, J = 15.0 Hz, 1H, benzyl CH_2), 3.39 (d, J = 15.0 Hz, 1H, benzyl CH_2), 2.29 (s, 3H, p-tol CH_3). ^{19}F NMR (376 MHz, THF-d_8, 25 °C): δ −118.45 (m, benzyl p-F).

■ ASSOCIATED CONTENT

Supporting Information

The Supporting Information is available free of charge on the ACS Publications website at DOI: 10.1021/acs.inorgchem.8b00079.

NMR, EPR, and UV/vis spectral data, description of 2D EXSY NMR and kinetic experiments, and details of computational studies (PDF)

■ AUTHOR INFORMATION

Corresponding Author

*E-mail: edwin.otten@rug.nl (E.O.).

ORCID

Edwin Otten: 0000-0002-5905-5108

Author Contributions

The manuscript was written through contributions of all authors. All authors have given approval to the final version of the manuscript.

Notes

The authors declare no competing financial interest.

■ ACKNOWLEDGMENTS

Financial support from The Netherlands Organisation for Scientific Research (NWO) is gratefully acknowledged (Vidi grant to E.O.).

■ REFERENCES

(1) Cook, T. R.; Dogutan, D. K.; Reece, S. Y.; Surendranath, Y.; Teets, T. S.; Nocera, D. G. Solar Energy Supply and Storage for the Legacy and Nonlegacy Worlds. *Chem. Rev.* **2010**, *110*, 6474.

(2) Appel, A. M.; Bercaw, J. E.; Bocarsly, A. B.; Dobbek, H.; DuBois, D. L.; Dupuis, M.; Ferry, J. G.; Fujita, E.; Hille, R.; Kenis, P. J. A.; Kerfeld, C. A.; Morris, R. H.; Peden, C. H. F.; Portis, A. R.; Ragsdale, S. W.; Rauchfuss, T. B.; Reek, J. N. H.; Seefeldt, L. C.; Thauer, R. K.; Waldrop, G. L. Frontiers, Opportunities, and Challenges in Biochemical and Chemical Catalysis of CO2 Fixation. *Chem. Rev.* **2013**, *113*, 6621.

(3) (a) Klerke, A.; Christensen, C. H.; Norskov, J. K.; Vegge, T. Ammonia for hydrogen storage: challenges and opportunities. *J. Mater. Chem.* **2008**, *18*, 2304. (b) Schuth, F.; Palkovits, R.; Schlogl, R.; Su, D. S. Ammonia as a possible element in an energy infrastructure: catalysts for ammonia decomposition. *Energy Environ. Sci.* **2012**, *5*, 6278.

(4) Roger, I.; Shipman, M. A.; Symes, M. D. Earth-abundant catalysts for electrochemical and photoelectrochemical water splitting. *Nat. Rev. Chem.* **2017**, *1*, 0003.

(5) Blakemore, J. D.; Crabtree, R. H.; Brudvig, G. W. Molecular Catalysts for Water Oxidation. *Chem. Rev.* **2015**, *115*, 12974.

(6) (a) Whittaker, J. W. Free Radical Catalysis by Galactose Oxidase. *Chem. Rev.* **2003**, *103*, 2347. (b) Lyons, C. T.; Stack, T. D. P. Recent advances in phenoxyl radical complexes of salen-type ligands as mixed-valent galactose oxidase models. *Coord. Chem. Rev.* **2013**, *257*, 528.

(7) Rittle, J.; Green, M. T. Cytochrome P450 Compound I: Capture, Characterization, and C-H Bond Activation Kinetics. *Science* **2010**, *330*, 933.

(8) (a) Dzik, W. I.; van der Vlugt, J. I.; Reek, J. N. H.; de Bruin, B. Ligands that Store and Release Electrons during Catalysis. *Angew. Chem., Int. Ed.* **2011**, *50*, 3356. (b) Lyaskovskyy, V.; de Bruin, B. Redox Non-Innocent Ligands: Versatile New Tools to Control Catalytic Reactions. *ACS Catal.* **2012**, *2*, 270. (c) Luca, O. R.; Crabtree, R. H. Redox-active ligands in catalysis. *Chem. Soc. Rev.* **2013**, *42*, 1440. (d) Broere, D. L. J.; Plessius, R.; van der Vlugt, J. I. New avenues for ligand-mediated processes - expanding metal reactivity by the use of redox-active catechol, o-aminophenol and o-phenylenediamine ligands. *Chem. Soc. Rev.* **2015**, *44*, 6886.

(9) (a) Römelt, C.; Song, J.; Tarrago, M.; Rees, J. A.; van Gastel, M.; Weyhermüller, T.; DeBeer, S.; Bill, E.; Neese, F.; Ye, S. Electronic Structure of a Formal Iron(0) Porphyrin Complex Relevant to CO2 Reduction. *Inorg. Chem.* **2017**, *56*, 4745. (b) Römelt, C.; Ye, S.; Bill, E.; Weyhermüller, T.; van Gastel, M.; Neese, F. Electronic Structure and Spin Multiplicity of Iron Tetraphenylporphyrins in Their Reduced States as Determined by a Combination of Resonance Raman Spectroscopy and Quantum Chemistry. *Inorg. Chem.* **2018**, DOI: 10.1021/acs.inorgchem.7b03018.

(10) Wu, Y.; Jiang, J.; Weng, Z.; Wang, M.; Broere, D. L. J.; Zhong, Y.; Brudvig, G. W.; Feng, Z.; Wang, H. Electroreduction of CO2 Catalyzed by a Heterogenized Zn−Porphyrin Complex with a Redox-Innocent Metal Center. *ACS Cent. Sci.* **2017**, *3*, 847.

(11) (a) Sengupta, D.; Bhattacharjee, R.; Pramanick, R.; Rath, S. P.; Saha Chowdhury, N.; Datta, A.; Goswami, S. Exclusively Ligand-Mediated Catalytic Dehydrogenation of Alcohols. *Inorg. Chem.* **2016**, *55*, 9602. (b) Sinha, S.; Das, S.; Sikari, R.; Parua, S.; Brandaõ, P.; Demeshko, S.; Meyer, F.; Paul, N. D. Redox Noninnocent Azo-Aromatic Pincers and Their Iron Complexes. Isolation, Characterization, and Catalytic Alcohol Oxidation. *Inorg. Chem.* **2017**, *56*, 14084.

(12) Schilter, D.; Camara, J. M.; Huynh, M. T.; Hammes-Schiffer, S.; Rauchfuss, T. B. Hydrogenase Enzymes and Their Synthetic Models: The Role of Metal Hydrides. *Chem. Rev.* **2016**, *116*, 8693.

(13) Dempsey, J. L.; Brunschwig, B. S.; Winkler, J. R.; Gray, H. B. Hydrogen Evolution Catalyzed by Cobaloximes. *Acc. Chem. Res.* **2009**, *42*, 1995.

(14) Kaeffer, N.; Chavarot-Kerlidou, M.; Artero, V. Hydrogen Evolution Catalyzed by Cobalt Diimine−Dioxime Complexes. *Acc. Chem. Res.* **2015**, *48*, 1286.

(15) (a) Bhattacharjee, A.; Chavarot-Kerlidou, M.; Andreiadis, E. S.; Fontecave, M.; Field, M. J.; Artero, V. Combined Experimental−Theoretical Characterization of the Hydrido-Cobaloxime [HCo(dmgH)2(PnBu3)]. *Inorg. Chem.* **2012**, *51*, 7087. (b) Estes, D. P.; Grills, D. C.; Norton, J. R. The Reaction of Cobaloximes with Hydrogen: Products and Thermodynamics. *J. Am. Chem. Soc.* **2014**, *136*, 17362. (c) Lacy, D. C.; Roberts, G. M.; Peters, J. C. The Cobalt Hydride that Never Was: Revisiting Schrauzer's "Hydridocobaloxime. *J. Am. Chem. Soc.* **2015**, *137*, 4860.

(16) Wiedner, E. S.; Bullock, R. M. Electrochemical Detection of Transient Cobalt Hydride Intermediates of Electrocatalytic Hydrogen Production. *J. Am. Chem. Soc.* **2016**, *138*, 8309.

(17) (a) Wilson, A. D.; Newell, R. H.; McNevin, M. J.; Muckerman, J. T.; Rakowski DuBois, M.; DuBois, D. L. Hydrogen Oxidation and Production Using Nickel-Based Molecular Catalysts with Positioned Proton Relays. *J. Am. Chem. Soc.* **2006**, *128*, 358. (b) Helm, M. L.; Stewart, M. P.; Bullock, R. M.; DuBois, M. R.; DuBois, D. L. A Synthetic Nickel Electrocatalyst with a Turnover Frequency Above 100,000 s^{-1} for H_2 Production. *Science* **2011**, *333*, 863. (c) Bullock, R. M.; Appel, A. M.; Helm, M. L. Production of hydrogen by electrocatalysis: making the H-H bond by combining protons and hydrides. *Chem. Commun.* **2014**, *50*, 3125.

(18) (a) McNamara, W. R.; Han, Z.; Alperin, P. J.; Brennessel, W. W.; Holland, P. L.; Eisenberg, R. A Cobalt−Dithiolene Complex for the Photocatalytic and Electrocatalytic Reduction of Protons. *J. Am. Chem. Soc.* **2011**, *133*, 15368. (b) McNamara, W. R.; Han, Z.; Yin, C.-J.; Brennessel, W. W.; Holland, P. L.; Eisenberg, R. Cobalt-dithiolene complexes for the photocatalytic and electrocatalytic reduction of protons in aqueous solutions. *Proc. Natl. Acad. Sci. U. S. A.* **2012**, *109*, 15594.

DOI: 10.1021/acs.inorgchem.8b00079
Inorg. Chem. 2018, 57, 9720−9727

(19) (a) Zarkadoulas, A.; Field, M. J.; Papatriantafyllopoulou, C.; Fize, J.; Artero, V.; Mitsopoulou, C. A. Experimental and Theoretical Insight into Electrocatalytic Hydrogen Evolution with Nickel Bis-(aryldithiolene) Complexes as Catalysts. *Inorg. Chem.* **2016**, *55*, 432. (b) Zarkadoulas, A.; Field, M. J.; Artero, V.; Mitsopoulou, C. A. Proton-Reduction Reaction Catalyzed by Homoleptic Nickel−bis-1,2-dithiolate Complexes: Experimental and Theoretical Mechanistic Investigations. *ChemCatChem* **2017**, *9*, 2308.

(20) Lee, K. J.; McCarthy, B. D.; Rountree, E. S.; Dempsey, J. L. Identification of an Electrode-Adsorbed Intermediate in the Catalytic Hydrogen Evolution Mechanism of a Cobalt Dithiolene Complex. *Inorg. Chem.* **2017**, *56*, 1988.

(21) (a) Downes, C. A.; Marinescu, S. C. Efficient Electrochemical and Photoelectrochemical H2 Production from Water by a Cobalt Dithiolene One-Dimensional Metal−Organic Surface. *J. Am. Chem. Soc.* **2015**, *137*, 13740. (b) Eady, S. C.; MacInnes, M. M.; Lehnert, N. Immobilized Cobalt Bis(benzenedithiolate) Complexes: Exceptionally Active Heterogeneous Electrocatalysts for Dihydrogen Production from Mildly Acidic Aqueous Solutions. *Inorg. Chem.* **2017**, *56*, 11654.

(22) (a) Solis, B. H.; Hammes-Schiffer, S. Computational Study of Anomalous Reduction Potentials for Hydrogen Evolution Catalyzed by Cobalt Dithiolene Complexes. *J. Am. Chem. Soc.* **2012**, *134*, 15253. (b) Letko, C. S.; Panetier, J. A.; Head-Gordon, M.; Tilley, T. D. Mechanism of the Electrocatalytic Reduction of Protons with Diaryldithiolene Cobalt Complexes. *J. Am. Chem. Soc.* **2014**, *136*, 9364. (c) Panetier, J. A.; Letko, C. S.; Tilley, T. D.; Head-Gordon, M. Computational Characterization of Redox Non-Innocence in Cobalt-Bis(Diaryldithiolene)-Catalyzed Proton Reduction. *J. Chem. Theory Comput.* **2016**, *12*, 223.

(23) (a) Haddad, A. Z.; Kumar, D.; Ouch Sampson, K.; Matzner, A. M.; Mashuta, M. S.; Grapperhaus, C. A. Proposed Ligand-Centered Electrocatalytic Hydrogen Evolution and Hydrogen Oxidation at a Noninnocent Mononuclear Metal−Thiolate. *J. Am. Chem. Soc.* **2015**, *137*, 9238. (b) Zhang, W.; Haddad, A. Z.; Garabato, B. D.; Kozlowski, P. M.; Buchanan, R. M.; Grapperhaus, C. A. Translation of Ligand-Centered Hydrogen Evolution Reaction Activity and Mechanism of a Rhenium-Thiolate from Solution to Modified Electrodes: A Combined Experimental and Density Functional Theory Study. *Inorg. Chem.* **2017**, *56*, 2177. (c) Haddad, A. Z.; Cronin, S. P.; Mashuta, M. S.; Buchanan, R. M.; Grapperhaus, C. A. Metal-Assisted Ligand-Centered Electrocatalytic Hydrogen Evolution upon Reduction of a Bis-(thiosemicarbazonato)Cu(II) Complex. *Inorg. Chem.* **2017**, *56*, 11254.

(24) (a) Solis, B. H.; Maher, A. G.; Dogutan, D. K.; Nocera, D. G.; Hammes-Schiffer, S. Nickel phlorin intermediate formed by proton-coupled electron transfer in hydrogen evolution mechanism. *Proc. Natl. Acad. Sci. U. S. A.* **2016**, *113*, 485. (b) Dempsey, J. L. Ligand steals spotlight from metal to orchestrate hydrogen production. *Proc. Natl. Acad. Sci. U. S. A.* **2016**, *113*, 478.

(25) (a) Thompson, E. J.; Berben, L. A. Electrocatalytic Hydrogen Production by an Aluminum(III) Complex: Ligand-Based Proton and Electron Transfer. *Angew. Chem., Int. Ed.* **2015**, *54*, 11642. (b) Sherbow, T. J.; Fettinger, J. C.; Berben, L. A. Control of Ligand pKa Values Tunes the Electrocatalytic Dihydrogen Evolution Mechanism in a Redox-Active Aluminum(III) Complex. *Inorg. Chem.* **2017**, *56*, 8651. (c) Haddad, A. Z.; Garabato, B. D.; Kozlowski, P. M.; Buchanan, R. M.; Grapperhaus, C. A. Beyond Metal-Hydrides: Non-Transition-Metal and Metal-Free Ligand-Centered Electrocatalytic Hydrogen Evolution and Hydrogen Oxidation. *J. Am. Chem. Soc.* **2016**, *138*, 7844. (d) Jiang, J.; Materna, K. L.; Hedström, S.; Yang, K. R.; Crabtree, R. H.; Batista, V. S.; Brudvig, G. W. Antimony Complexes for Electrocatalysis: Activity of a Main-Group Element in Proton Reduction. *Angew. Chem., Int. Ed.* **2017**, *56*, 9111. (e) For a review on main-group compounds showing transition-metal-like reactivity, see: Power, P. P. *Nature* **2010**, *463*, 171.

(26) (a) Gilroy, J. B.; Ferguson, M. J.; McDonald, R.; Patrick, B. O.; Hicks, R. G. Formazans as β-diketiminate analogues. Structural characterization of boratatetrazines and their reduction to borataverdazyl radical anions. *Chem. Commun.* **2007**, 126. (b) Gilroy, J. B.; Ferguson, M. J.; McDonald, R.; Hicks, R. G. Synthesis and characterization of palladium complexes of 3-nitroformazans. *Inorg. Chim. Acta* **2008**, *361*, 3388. (c) Gilroy, J. B.; Patrick, B. O.; McDonald, R.; Hicks, R. G. Transition Metal Complexes of 3-Cyano- and 3-Nitroformazans. *Inorg. Chem.* **2008**, *47*, 1287. (d) Gilroy, J. B.; Otieno, P. O.; Ferguson, M. J.; McDonald, R.; Hicks, R. G. Synthesis and Characterization of 3-Cyano- and 3-Nitroformazans, Nitrogen-Rich Analogues of β-Diketimine Ligands. *Inorg. Chem.* **2008**, *47*, 1279. (e) Hong, S.; Hill, L. M. R.; Gupta, A. K.; Naab, B. D.; Gilroy, J. B.; Hicks, R. G.; Cramer, C. J.; Tolman, W. B. Effects of Electron-Deficient β-Diketiminate and Formazan Supporting Ligands on Copper(I)-Mediated Dioxygen Activation. *Inorg. Chem.* **2009**, *48*, 4514.

(27) Chang, M.-C.; Dann, T.; Day, D. P.; Lutz, M.; Wildgoose, G. G.; Otten, E. The Formazanate Ligand as an Electron Reservoir: Bis(Formazanate) Zinc Complexes Isolated in Three Redox States. *Angew. Chem., Int. Ed.* **2014**, *53*, 4118.

(28) For a review, see: Sigeikin, G. I.; Lipunova, G. N.; Pervova, I. G. Formazans and their metal complexes. *Russ. Chem. Rev.* **2006**, *75*, 885.

(29) (a) Beffa, F.; Lienhard, P.; Steiner, E.; Schetty, G. Über isomere 1:2-Kobaltkomplexe der Formazan-Reihe. *Helv. Chim. Acta* **1963**, *46*, 1369. (b) Dale, D. The X-ray crystallographic determination of the structure of di-[3-methyl-1(or 5)-phenyl-5(or 1)-p-tolylformazyl]-nickel(II). *J. Chem. Soc. A* **1967**, 278. (c) Balt, S.; Renkema, W. E. Electron paramagnetic resonance study of coordination in formazan copper(II) complexes. *J. Coord. Chem.* **1977**, *6*, 201. (d) Renkema, W. E.; Lute, C. N.; Stam, C. H. Ammine[1-(2-hydroxyphenyl)-3,5-diphenylformazanato]copper(II), C19H17CuIIN5O, and ammine[1-(2-hydroxyphenyl)-3,5-diphenylformazanato]nickel(II), C19H17N5NiIIO. *Acta Crystallogr., Sect. B: Struct. Crystallogr. Cryst. Chem.* **1979**, *35*, 75. (e) Bait, S.; Meuldijk, J.; Renkema, W. Square planar complexes of nickel(II), palladium(II) and platinum(II) with 1-(2-hydroxyphenyl)-3,5-diphenylformazan. *Transition Met. Chem.* **1980**, *5*, 357. (f) Siedle, A. R.; Pignolet, L. H. Formazanylpalladium compounds. Synthesis and structure of bis(1,3,5-tri-p-tolylformazanyl)palladium. *Inorg. Chem.* **1980**, *19*, 2052. (g) Jameson, G. B.; Muster, A.; Robinson, S. D.; Wingfield, J. N.; Ibers, J. A. Cyclometalated formazan derivatives of ruthenium and osmium: structure of Ru((o-C6H4)N:NC(Ph):NNPh)(CO)(PPh3)2. *Inorg. Chem.* **1981**, *20*, 2448. (h) Meuldijk, J.; Renkema, W. E.; van Herk, A. M.; Stam, C. H. Ammine[1-(2-hydroxyphenyl)-3,5-diphenylformazanato]nickel(II), [Ni(C19H14N4O)(NH3)], and [1-(2-hydroxyphenyl)-5-phenyl-3-(p-tolyl)formazanato](pyridine)nickel-(II), [Ni(C5H5N)(C20H16N4O)]. *Acta Crystallogr., Sect. C: Cryst. Struct. Commun.* **1983**, *39*, 1536. (i) Kawamura, Y.; Yamauchi, J. ESR Study of Paramagnetic Nickel Species Obtained by Reduction and Oxidation of Bis(1,3,5-triphenylformazanato)nickel(II). *Bull. Chem. Soc. Jpn.* **1995**, *68*, 3041. (j) Zhang, H.-Y.; Sun, W.-X.; Wu, Q.-A.; Zhangb, H.-Q.; Chen, Y.-Y. Study on 1,5-Bis(2-carboxyphenyl)-3-phenylformazan and its Complexes. *Synth. React. Inorg. Met.-Org. Chem.* **2000**, *30*, 571. (k) Frolova, N.; Vatsadze, S.; Zavodnik, V.; Rakhimov, R.; Zyk, N. Pyridine-containing nickel(II) bis-formazanates: Synthesis, structure, and electrochemical study. *Russ. Chem. Bull.* **2006**, *55*, 1810.

(30) (a) Barbon, S. M.; Reinkeluers, P. A.; Price, J. T.; Staroverov, V. N.; Gilroy, J. B. Structurally Tunable 3-Cyanoformazanate Boron Difluoride Dyes. *Chem. - Eur. J.* **2014**, *20*, 11340. (b) Barbon, S. M.; Price, J. T.; Reinkeluers, P. A.; Gilroy, J. B. Substituent-Dependent Optical and Electrochemical Properties of Triarylformazanate Boron Difluoride Complexes. *Inorg. Chem.* **2014**, *53*, 10585. (c) Maar, R. R.; Barbon, S. M.; Sharma, N.; Groom, H.; Luyt, L. G.; Gilroy, J. B. Evaluation of Anisole-Substituted Boron Difluoride Formazanate Complexes for Fluorescence Cell Imaging. *Chem. - Eur. J.* **2015**, *21*, 15589. (d) Hesari, M.; Barbon, S. M.; Staroverov, V. N.; Ding, Z.; Gilroy, J. B. Efficient electrochemiluminescence of a readily accessible boron difluoride formazanate dye. *Chem. Commun.* **2015**, *51*, 3766. (e) Barbon, S. M.; Staroverov, V. N.; Gilroy, J. B. Effect of Extended π Conjugation on the Spectroscopic and Electrochemical Properties of Boron Difluoride Formazanate Complexes. *J. Org. Chem.* **2015**, *80*, 5226. (f) Barbon, S. M.; Price, J. T.; Yogarajah, U.; Gilroy, J. B.

DOI: 10.1021/acs.inorgchem.8b00079
Inorg. Chem. 2018, 57, 9720−9727

Synthesis and characterization of conjugated/cross-conjugated benzene-bridged boron difluoride formazanate dimers. *RSC Adv.* **2015**, *5*, 56316. (g) Maar, R. R.; Gilroy, J. B. Aggregation-induced emission enhancement in boron difluoride complexes of 3-cyanoformazanates. *J. Mater. Chem. C* **2016**, *4*, 6478. (h) Maar, R. R.; Rabiee Kenaree, A.; Zhang, R.; Tao, Y.; Katzman, B. D.; Staroverov, V. N.; Ding, Z.; Gilroy, J. B. Aluminum Complexes of N2O23− Formazanate Ligands Supported by Phosphine Oxide Donors. *Inorg. Chem.* **2017**, *56*, 12436. (i) Barbon, S. M.; Staroverov, V. N.; Gilroy, J. B. Structurally Diverse Boron−Nitrogen Heterocycles from an N2O23− Formazanate Ligand. *Angew. Chem., Int. Ed.* **2017**, *56*, 8173. (j) Barbon, S. M.; Buddingh, J. V.; Maar, R. R.; Gilroy, J. B. Boron Difluoride Adducts of a Flexidentate Pyridine-Substituted Formazanate Ligand: Property Modulation via Protonation and Coordination Chemistry. *Inorg. Chem.* **2017**, *56*, 12003.

(31) (a) Tezcan, H.; Uzluk, E.; Aksu, M. L. Electrochemical and spectroscopic properties of 1:2 Ni complexes of 1,3-substitued (CH3, OCH3) phenyl-5-phenylformazans. *Electrochim. Acta* **2008**, *53*, 5597. (b) Zaidman, A. V.; Pervova, I. G.; Vilms, A. I.; Belov, G. P.; Kayumov, R. R.; Slepukhin, P. A.; Lipunov, I. N. Synthesis, characterization and ethylene oligomerization studies of nickel(II) based new formazane derivatives. *Inorg. Chim. Acta* **2011**, *367*, 29. (c) Protasenko, N. A.; Poddel'sky, A. I.; Bogomyakov, A. S.; Fukin, G. K.; Cherkasov, V. K. Heteroligand o-Semiquinonato-Formazanato Cobalt Complexes. *Inorg. Chem.* **2015**, *54*, 6078. (d) Mandal, A.; Schwederski, B.; Fiedler, J.; Kaim, W.; Lahiri, G. K. Evidence for Bidirectional Noninnocent Behavior of a Formazanate Ligand in Ruthenium Complexes. *Inorg. Chem.* **2015**, *54*, 8126. (e) Kabir, E.; Wu, C.-H.; Wu, J. I. C.; Teets, T. S. Heteroleptic Complexes of Cyclometalated Platinum with Triarylformazanate Ligands. *Inorg. Chem.* **2016**, *55*, 956. (f) Schorn, W.; Grosse-Hagenbrock, D.; Oelkers, B.; Sundermeyer, J. Formazanido complexes of heavier group 13 elements aluminium, gallium, and indium. *Dalton Trans.* **2016**, *45*, 1201.

(32) (a) Novoa, S.; Paquette, J. A.; Barbon, S. M.; Maar, R. R.; Gilroy, J. B. Side-chain boron difluoride formazanate polymers via ring-opening metathesis polymerization. *J. Mater. Chem. C* **2016**, *4*, 3987. (b) Barbon, S. M.; Gilroy, J. B. Boron difluoride formazanate copolymers with 9,9-di-n-hexylfluorene prepared by copper-catalyzed alkyne-azide cycloaddition chemistry. *Polym. Chem.* **2016**, *7*, 3589. (c) Barbon, S. M.; Novoa, S.; Bender, D.; Groom, H.; Luyt, L. G.; Gilroy, J. B. Copper-assisted azide-alkyne cycloaddition chemistry as a tool for the production of emissive boron difluoride 3-cyanoformazanates. *Org. Chem. Front.* **2017**, *4*, 178. (d) Novoa, S.; Gilroy, J. B. (Co)polymers containing boron difluoride 3-cyanoformazanate complexes: emission enhancement via random copolymerization. *Polym. Chem.* **2017**, *8*, 5388.

(33) (a) Chang, M. C.; Otten, E. Synthesis and ligand-based reduction chemistry of boron difluoride complexes with redox-active formazanate ligands. *Chem. Commun.* **2014**, *50*, 7431. (b) Chang, M. C.; Chantzis, A.; Jacquemin, D.; Otten, E. Boron difluorides with formazanate ligands: redox-switchable fluorescent dyes with large stokes shifts. *Dalton Transactions* **2016**, *45*, 9477. (c) Mondol, R.; Snoeken, D. A.; Chang, M.-C.; Otten, E. Stable, crystalline boron complexes with mono-, di- and trianionic formazanate ligands. *Chem. Commun.* **2017**, *53*, 513.

(34) Chang, M.-C.; Otten, E. Reduction of (Formazanate)boron Difluoride Provides Evidence for an N-Heterocyclic B(I) Carbenoid Intermediate. *Inorg. Chem.* **2015**, *54*, 8656.

(35) (a) Matuschek, D.; Eusterwiemann, S.; Stegemann, L.; Doerenkamp, C.; Wibbeling, B.; Daniliuc, C. G.; Doltsinis, N. L.; Strassert, C. A.; Eckert, H.; Studer, A. Profluorescent verdazyl radicals - synthesis and characterization. *Chem. Sci.* **2015**, *6*, 4712. (b) Hicks, R. G. *Stable Radicals*; John Wiley & Sons, Ltd., 2010; p 245.

(36) Chang, M.-C.; Otten, E. Intramolecular Hydride Transfer Reactions in (Formazanate)Boron Dihydride Complexes. *Organometallics* **2016**, *35*, 534.

(37) Johnston, C. W.; Schwantje, T. R.; Ferguson, M. J.; McDonald, R.; Hicks, R. G. Metal coordination, and metal-ligand redox noninnocence, modulates allosteric C-N bond homolysis in an N-benzyl tetrazine. *Chem. Commun.* **2014**, *50*, 12542.

(38) (a) Polumbrik, O.; Ryabokon, I. Strength of NH bond in 2,4,6-triphenyl-1,2,3,4-tetrahydrosym-tetrazine (leucoverdazyl). *Zh. Org. Khim.* **1978**, *14*, 1332. (b) Misyura, A.; Polumbrik, O.; Markovskii, L. Energy of NH bond dissociation in 2,6-diaryl-4-phenyl-1,2,3,4,-tetrahydro-sym-tetrazines and comparative activity of sym-tetrazinyls in the reaction of hydrazobenzene dehydrogenation. *Zh. Org. Khim.* **1989**, *25*, 424.

(39) Warren, J. J.; Tronic, T. A.; Mayer, J. M. Thermochemistry of Proton-Coupled Electron Transfer Reagents and its Implications. *Chem. Rev.* **2010**, *110*, 6961.

(40) (a) Skene, W. G.; Belt, S. T.; Connolly, T. J.; Hahn, P.; Scaiano, J. C. Decomposition Kinetics, Arrhenius Parameters, and Bond Dissociation Energies for Alkoxyamines of Relevance in "Living" Free Radical Polymerization. *Macromolecules* **1998**, *31*, 9103. (b) Marque, S.; Le Mercier, C.; Tordo, P.; Fischer, H. Factors Influencing the C−O−Bond Homolysis of Trialkylhydroxylamines. *Macromolecules* **2000**, *33*, 4403.

(41) Lukkarila, J. L. Ph.D. Thesis, University of Toronto, Toronto, Canada, 2009.

(42) (a) Marsal, P.; Roche, M.; Tordo, P.; de Sainte Claire, P. Thermal Stability of O−H and O−Alkyl Bonds in N-Alkoxyamines. A Density Functional Theory Approach. *J. Phys. Chem. A* **1999**, *103*, 2899. (b) Gaudel-Siri, A.; Siri, D.; Tordo, P. Homolysis of N-alkoxyamines: A Computational Study. *ChemPhysChem* **2006**, *7*, 430.

(43) Huang, K.-W.; Han, J. H.; Cole, A. P.; Musgrave, C. B.; Waymouth, R. M. Homolysis of Weak Ti−O Bonds: Experimental and Theoretical Studies of Titanium Oxygen Bonds Derived from Stable Nitroxyl Radicals. *J. Am. Chem. Soc.* **2005**, *127*, 3807.

DOI: 10.1021/acs.inorgchem.8b00079
Inorg. Chem. 2018, 57, 9720−9727